MOLECULAR DYNAMICS SIMULATION OF WATER VAPOR CONDENSATION ON NANOSTRUCTURED SURFACES

Yingjie Tan [1], Hui Jiang [2 *], Yang Sun [1], Huanyu Zhang [3]

[1] School of Architecture, Liaoning Vocational University of Technology, Jinzhou, China

[2] School of Energy and Power Engineering, Guangdong University of Petrochemical Technology, Maoming, China

[3] China Petroleum Pipeline Bureau Engineering Company Limited, Langfang, China

* Corresponding author, Email: jianghui@gdupt.edu.cn

The frosting of the air source heat pump evaporator reduces the system heating efficiency. Compared to active defrosting, utilizing passive methods such as superhydrophobic surfaces to inhibit defrosting can effectively reduce power consumption. In this paper, the condensation nucleation of water vapor on the copper surface with nanostructures was simulated by molecular dynamics. The effect of solid-liquid interaction strength on the nucleation characteristics at the early stage of frost formation was analyzed. The results show that as solid-liquid interaction strength increases, the condensate droplets evolve from Cassie to Wenzel state, which promotes the frosting process of the droplets. The process of Wenzel state droplets merging to form the Cassie state was found due to the combination of surface free energy and nanostructure. The transition mechanism of the droplet wetting state is revealed through the distribution of potential energy on the nanostructure surface. The area and value of the low potential energy region near the nanostructure surface increases with the solid-liquid interaction strength, which enhances the attraction of the surface to water molecules.

Key words*: Air Source Heat pumps, Molecular Dynamics, Wettability, Condensation, Nanostructure*

1. Introduction

The air-source heat pump is widely used in various buildings as the cold and heat source of air conditioning systems due to its high efficiency, energy saving, and environmental protection [1, 2]. However, for the actual application process, the efficiency of the air source heat pump is not ideal. During the air source heat pump operation in winter, the evaporator inevitably frosts [3]. Some studies show that the accumulated frost layer will reduce the efficiency by nearly 30% and even cause the heat pump unit to break down [4, 5]. To solve the frost formation problem, Hayashi et al. [6] observed the frost formation process of the whole stainless steel plate, the frost formation process is roughly divided into three stages, frost crystal growth period, frost layer growth period, and frost layer complete growth period. For the frost crystal growth period (the initial frost), when the water vapor in the air contact with cold surface of the evaporator, it can form condensation nuclei and grow into droplets. For the frost growth phase, the droplets transform into dendritic frost crystals, which gradually develop into a thicker frost layers. Since active defrosting methods (such as heating) are difficult to fundamentally solve the frosting problem of air source heat pumps, those methods can increase energy consumption [7, 8]. The key to solving the frosting problem is to effectively inhibit the condensation and nucleation of water

vapor at the initial stage of frosting.

Inspired by the “lotus leaf effect”, scholars applied a superhydrophobic surface to inhibit the condensation and nucleation of water vapor [9-11]. Some studies found that during the wetting process of droplets on the superhydrophobic surface, the merged droplets release surface energy and make them jump off the surface [12-14]. So passive methods such as superhydrophobic surface provides new ideas to inhibit frosting at the initial stage. However, due to the limitations of experimental conditions, when the characteristic scale of the droplet is nanoscale, the condensation and nucleation of water vapor on the superhydrophobic nanostructure surface are not clear. The scale effect may have an important effect on droplet nucleation processes.

With the development of computer science in recent decades, molecular dynamics simulation has become an essential tool for studying the condensation and nucleation of water vapor on a molecular scale. Several studies discussed the effect of different nanostructures on condensation. For example, Hiratsuka et al. [15] explored the effect of the height of square column nanostructure on water vapor condensation through molecular dynamics. Liu et al. [16] investigated the condensation on three different shapes of copper nanoarrays surface under actual working conditions. They found that the prismatic cone matrix structure has the strongest inhibition effect on water vapor condensation. Some studies have focused on surface wettability. Fujii et al. [17] investigated the effect of nanostructure parameters with different surface wettability on argon condensation. They found that the Lennard-Jones (LJ) potential energy parameters can change surface hydrophobicity, thus affecting the condensation behavior of argon vapor. Considering the role of the hydrophilic surface and hydrophobic surface, the mixed wettability surfaces were analysed. Wang et al. [18] studied the condensation behavior on the hydrophobic surface with hydrophilic points. They found that preferential nucleation of droplets occurs in the hydrophilic point region. Paul et al. [19] further investigated the effect of the proportion of hydrophobic regions on the condensation behavior for mixed wettability surfaces.

In summary, most studies on condensation have focused on single nanostructure surfaces or mixed wettability smooth surfaces. There are few reports about condensation processes on nanostructure surfaces with different surface wettability [17]. In this study, the molecular dynamics simulation was used to explore the effect of solid-liquid interaction strength on condensation in the early frosting stage on the square-column nanostructure surface. The cluster’s behavior under solid-liquid interaction strength was analyzed. Furthermore, the relationship between the potential energy distribution and droplet wetting state was revealed.

2. Simulation method

The effects of solid-liquid interaction strength on condensation nucleation were studied by molecular dynamics. The condensation model is shown in Fig. 1(a). The size of the simulation system was $L_x \times L_y \times L_z$=6.5 nm×6.5 nm×21 nm. Referring to our previous work [16], the bottom of the simulation system is the square-columnar nanostructure wall for condensation. The dimensions of the square-columnar nanostructure are shown in Fig. 1(b). The top region is the smooth wall for heating water molecules. The liquid phase water is located near the heated wall. The solid wall consists of copper atoms with face-centered cube lattice arrangement. The lattice parameter a_{cu}=0.361 nm [20]. The number of water molecules is set as 5000 to balance computational efficiency and accuracy. The periodic boundary was used in the *x* and *y* directions, and the fixed boundary was used in the *z* directions.

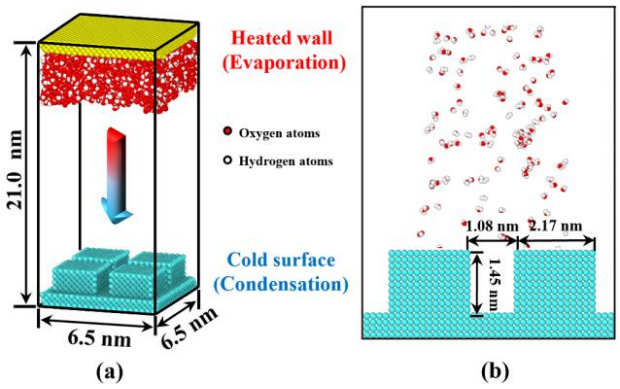

Fig. 1. Condensation model of water vapor on copper nanostructure wall. (a) Simulation system. (b) Square-columnar nanostructure.

The interaction between water molecules is described by TIP4P/2005 model [21], which is widely used to simulate the condensation process due to the accurate thermodynamic and structural properties.

$$\phi\left(r_{ij}\right)=4\varepsilon\left[\left(\frac{\sigma}{r_{ij}}\right)^{12}-\left(\frac{\sigma}{r_{ij}}\right)^{6}\right]+\frac{q_i q_j}{4\pi\varepsilon_0 r_{ij}} \tag{1}$$

where σ is the size parameter, σ_O=0.31589 nm, ε is the energy parameter, ε_O=0.00803 eV, r is the distance between any two atoms, q is the charge, q_O=-1.1128 e, q_H=0.5564 e, and ε_0 is the vacuum dielectric constant.

The interaction between copper atoms is described by EAM model [22]. The interaction between solid and liquid atoms is described by LJ model [16].

$$\phi\left(r_{ij}\right)=4\varepsilon_{\text{Cu-O}}\left[\left(\frac{\sigma_{\text{Cu-O}}}{r_{ij}}\right)^{12}-\left(\frac{\sigma_{\text{Cu-O}}}{r_{ij}}\right)^{6}\right] \tag{2}$$

where $\sigma_{\text{Cu-O}}$ and $\varepsilon_{\text{Cu-O}}$ are the size parameter and energy parameter of copper atom and oxygen atom. $\sigma_{\text{Cu-O}}$ can be obtain by Lorentz-Berthelot relationship, $\sigma_{\text{Cu-O}}=(\sigma_{\text{Cu}}+\sigma_O)/2$=0.275 nm. In order to obtain different fluid-solid interaction strengths, $\varepsilon_{\text{Cu-O}}$ was adjusted. Here, parameter f was introduced. $\varepsilon_{\text{Cu-O}}$ corresponding to different f is shown in Table 1.

$$f=\frac{\varepsilon_{\text{Cu-O}}}{\varepsilon_O} \tag{3}$$

The open-source software LAMMPS is used for molecular dynamics simulation [23], and the OVITO is used to observe atomic trajectories of condensation. In the simulation, the Verlet algorithm [24] integrated Newton's equation of motion. The time step is 1.0 fs. The truncation radius of LJ interaction and Coulomb interaction is 1.2 nm. The Long-range Coulomb forces were calculated using PPPM [25]. The SHAKE algorithm [26] was used to fix the bond length and angle of water molecules. First, the whole system was relaxed at a temperature of 300 K by the Nose-Hoover thermostat in the NVT ensemble. After 1 ns, the temperature of the smooth wall increases to 400 K for heating water molecules, and the nanostructure wall remains at 300 K. The temperature control of the water molecules is removed and the NVE ensemble is applied to the whole system. The condensation process lasts 10 ns to obtain the final droplet wetting state.

Table 1. The $\varepsilon_{Cu\text{-}O}$ corresponding to different f

f	1.0	1.2	1.4	1.6
$\varepsilon_{Cu\text{-}O}$	0.007058	0.008470	0.009881	0.011293

3. Results and discussions

Fig. 2 shows the condensation process of water vapor on nanostructure surfaces under different fluid-solid interaction strengths. In the initial moments, individual water molecules are dispersed in the gas phase space above the nanostructure surface. As the heating of top wall, more water molecules leave the top region and move to the gas phase space in the middle region. When gas phase water molecules are close to the nanostructure surface, the temperature of water molecules decreases due to the cooling of the nanostructure wall. Water molecules tend to aggregate and form clusters on the cold surface. If the distance between the oxygen atoms in each water molecule is less than $1.5\sigma_O$, they are considered to belong to a cluster. As the clusters merge to eventually form droplets with different wetting states, depends on the fluid-solid interaction strength. For the weak fluid-solid interaction strength (f=1.0), most water molecules appear in the gas phase space, and do not condense on the nanostructure surface due to the superhydrophobicity. As the fluid-solid interaction strength increases (f=1.2), few water molecules condense on the top of nanopillars. For f=1.4, a small cluster forms in the gap of nanopillars at 2 ns. The small cluster grows gradually to form a Wenzel state droplet at 4 ns. At 6 ns, the droplet escapes from the confinement of nanopillars and moves upwards with the transition from Wenzel state to Cassie state.

Similarly, the theoretical calculations and experimental verification by He et al [27] also show the droplets on the nanostructure surface may undergo a transition from Wenzel to Cassie state due to the release of surface free energy. The droplets need to reach a critical diameter on the superhydrophobic surface to break the energy barrier for the wetting state transition. With the increase of fluid-solid interaction strength (f=1.6), small clusters also form in the gap of nanopillars. But the droplet keeps growing with Wenzel state until the end of the simulation.

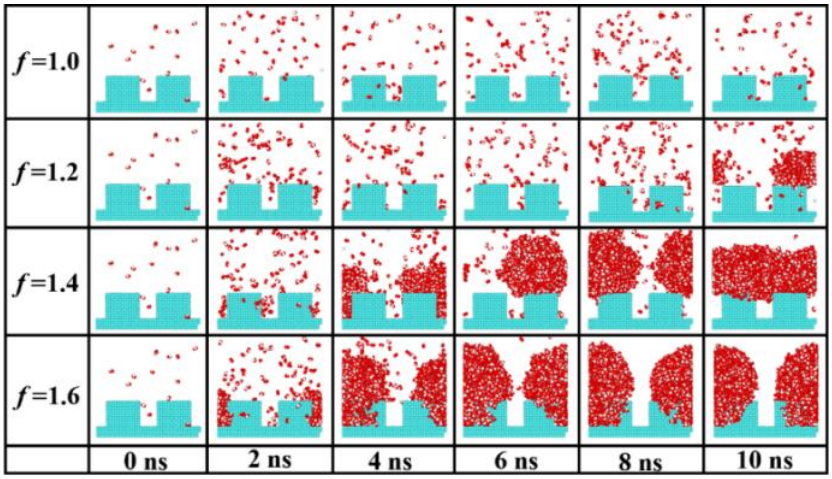

Fig. 2. The condensation process of water vapour on the surface of the nanostructures under different fluid-solid interaction strengths.

From the condensation process of water vapor on the nanostructure surface in Fig. 2, in which the cluster's behavior has a significant effect on the final droplet wetting state. Fig. 3 shows the number of

clusters in the entire simulation domain. The number of clusters under different fluid-solid interaction strength was analyzed. The data of the number of clusters with time are fitted by the polynomial. Except for the weak fluid-solid interaction strength (f=1.0), the number of clusters first increases and then decreases. When the top wall heats the liquid phase water, the number of gas phase water molecules increases, leading to an increasing number of clusters. When the gas phase water molecules condense on the nanostructure surface, the initial liquid droplet is formed. As the droplets grow and merge, the number of clusters decreases. For f=1.2, most water molecules remain in the gas phase above the nanostructure surface at t=2~8 ns (see Fig. 2), so the number of clusters remains stable. As water vapor condenses at the top of the nanopillar, the number of clusters decreases. As the strength of fluid-solid interaction increases, the water vapor condenses early, and the number of clusters declines more rapidly. For f=1.4, the cluster number drop to 0 occurs at 10 ns. For f=1.6, the clusters number drop to 0 occurs at 6 ns. The small cluster number in the late stages of condensation represent a larger droplet. For f=1.0, most water molecules exist in the gas phase without condensation phenomena, so the number of clusters remains stable.

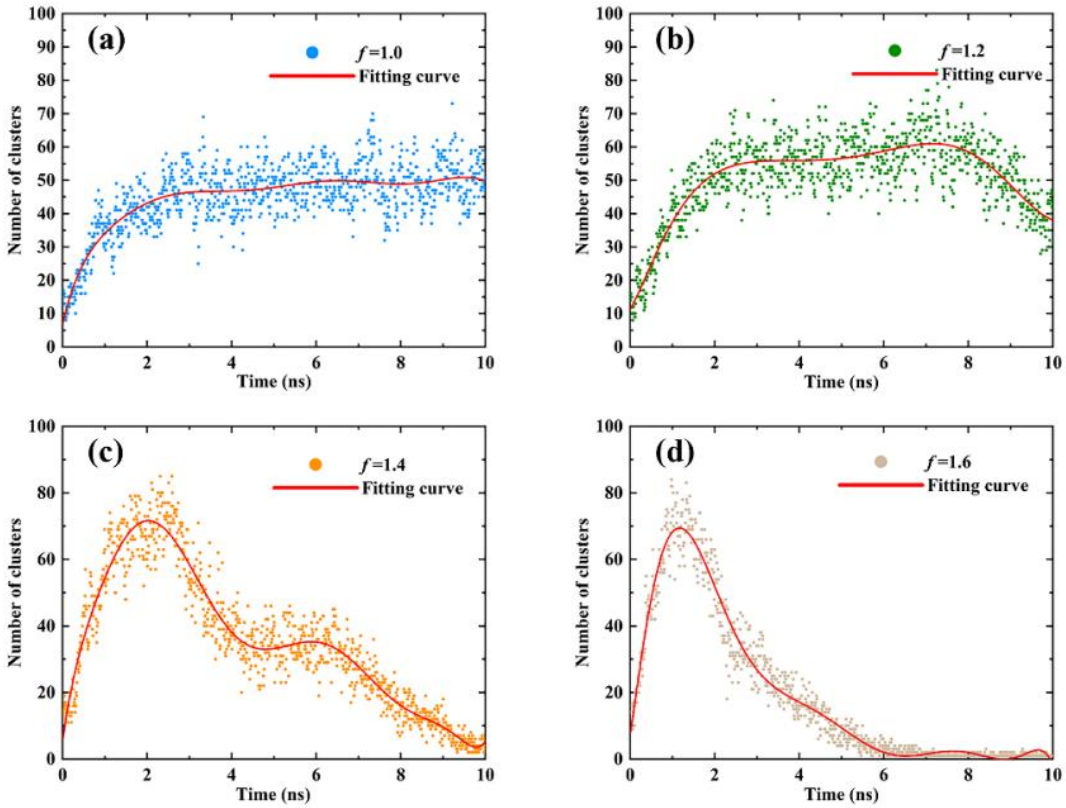

Fig. 3. The variation of clusters numbers with time under different fluid-solid interaction strengths. (a) f=1.0, (b) f=1.2, (c) f=1.4, (d) f=1.6.

In addition, the variation of the maximum size of clusters under different fluid-solid interaction strengths was analyzed. In this paper, the size of clusters represents the number of water molecules in this cluster. As shown in Fig. 4, except for f=1.0, the maximum size of clusters increases with time. For f=1.2, the maximum size of clusters increases at 8 ns, which is consistent with the variation of cluster number in Fig. 3. For f=1.4 and f=1.6, the curve suddenly rises at t=8.9 ns and t=1.7 ns, which indicates the merger between several clusters rather than direct condensation of vapor molecules. For f=1.0, the maximum size of clusters oscillates between 3~5 due to the lack of condensation of water vapor.

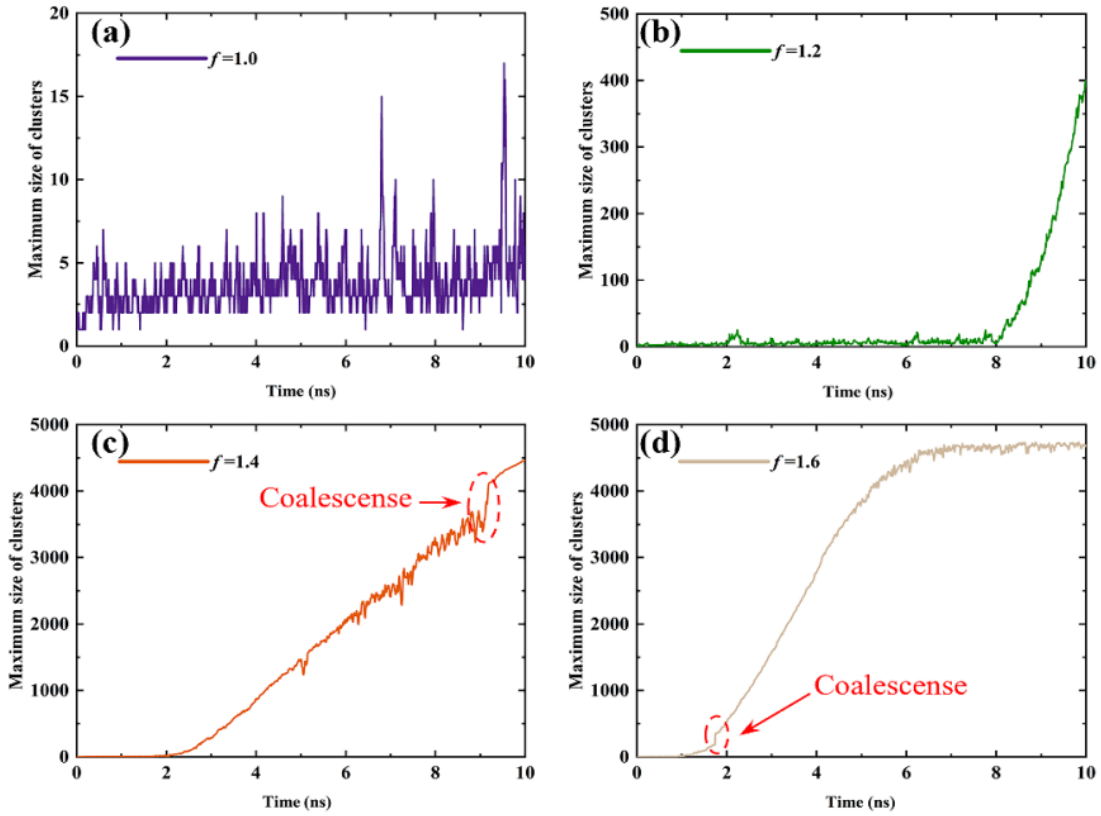

Fig. 4. The variation of maximum cluster size with time under different fluid-solid interaction strengths. (a) *f*=1.0, (b) *f*=1.2, (c) *f*=1.4, (d) *f*=1.6.

Fig. 5 shows the number of condensed molecules on the nanostructure surface under different fluid-solid interaction strengths. As the fluid-solid interaction strength increases, the number of condensed molecules increases with time, caused by the strong wall attraction. Compared to *f*=1.0 and *f*=1.2, *f*=1.4 and *f*=1.6 cases significantly increases the condensation rate, resulting in a larger droplet. The above analysis of the number and maximum size of clusters is consistent with the condensation process shown in Fig. 2.

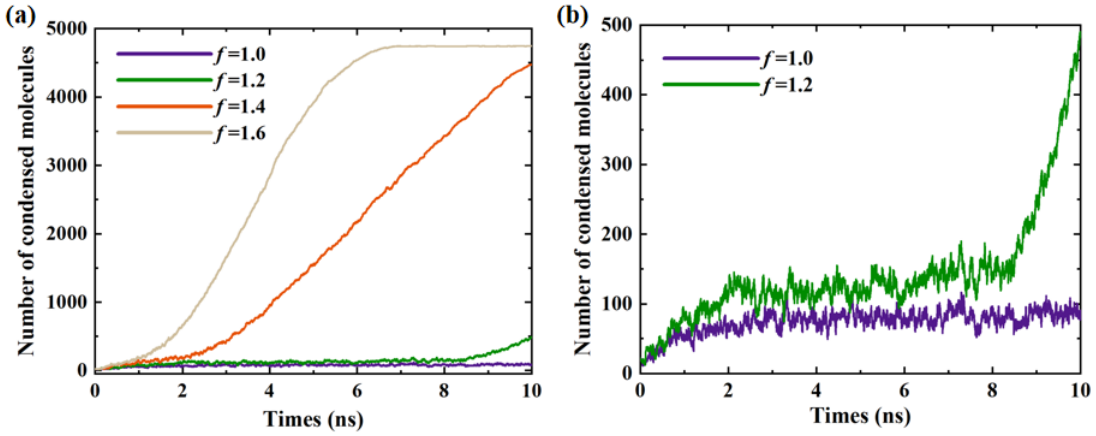

Fig. 5. The variation of the number of condensed molecules with time under different fluid-solid interaction strengths. (a) For fluid-solid interaction strength *f*=1.0~1.6. (b) Enlarged image at *f*=1.0 and *f*=1.2.

Fig. 6 shows the density distribution of water molecules along the *z*-direction under different fluid-solid interaction strengths. Statistical density distribution regions include the near-wall region and

droplet region. For *f*=1.0~1.6, the density distribution in the gap of nanopillars is close to 0, indicating the absence of droplet condensation and Cassie state wetting, respectively. For *f*=1.6, the obvious density peak occurs in the gap of the nanopillar, which represents the appearance of the Wenzel state droplet in the nanostructural gap due to strong fluid-solid interaction. For the droplet region, a small droplet form at *f*=1.2, and a big droplet form at *f*=1.4~1.6.

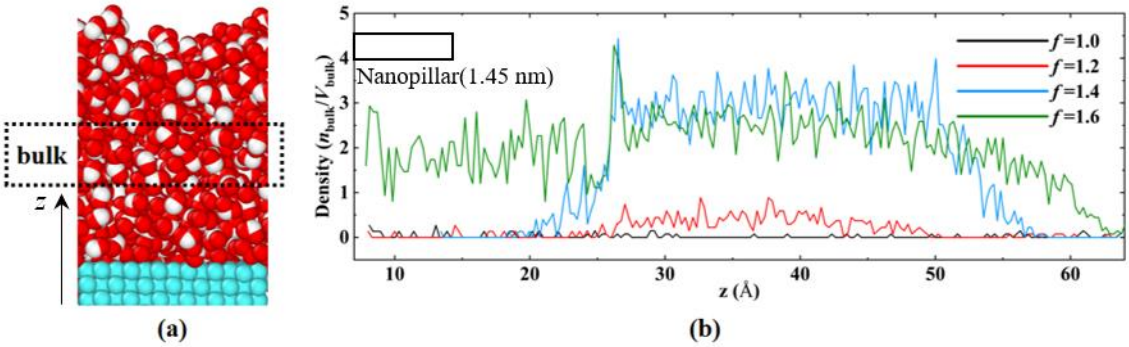

Fig. 6. The density distribution of water molecules along the *z*-direction. (a) Schematic diagram of water density along the *z* direction. (b) Density distribution under different fluid-solid interaction strengths.

To further reveal the wetting state under different fluid-solid interaction strengths, the effect of potential energy on the nucleation process is analyzed. Fig. 7 shows the variation of potential energy between the oxygen atom and copper atom with distance under different fluid-solid interaction strengths. As surface wettability increases, potential energy wells that form from fluid-solid interaction are deeper, leading to a tendency for vapor molecules to nucleate on the nanostructure surface.

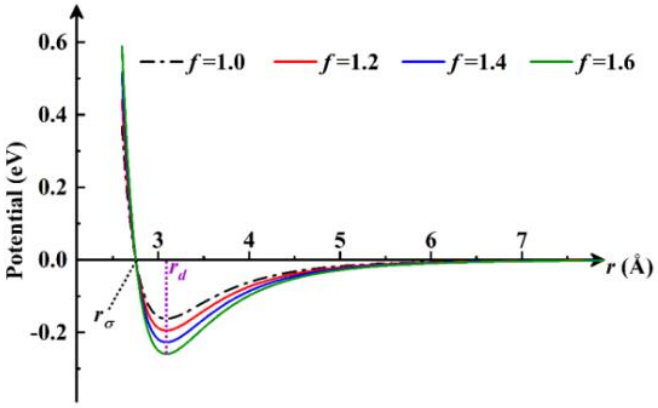

Fig. 7. LJ potential energy curves under different fluid-solid interaction strengths.

To analyze the effect of the nanopillar on the wetting state of the droplets, the potential energy distribution along the cross-section is shown in Fig. 8. The potential energy away from the solid wall approaches 0, indicating that the wall only affects the near-wall fluid. The area and value of low potential regions increase with fluid-solid interaction strength, leading the wetting transition from *f*=1.2 to *f*=1.6. There are two low potential regions in the gap of nanopillar. A similar result is also obtained by Gao et al [28], which shows that the potential energy calculation in this simulation is reasonable. Compared to the top region of the nanopillar, the potential energy of the nanopillars gap is lower, resulting in a stronger attraction to vapor molecules. So gas phase molecules preferentially nucleate in the nanostructural gap and form the Wenzel state droplet. For *f*=1.4, the Wenzel state droplets first appear in the nanostructural gap and then merge to release energy to break through the nanostructural confines.

The droplet moves towards another low potential energy region at the top of the nanopillars, leading to the transition from the Wenzel state to the Cassie state.

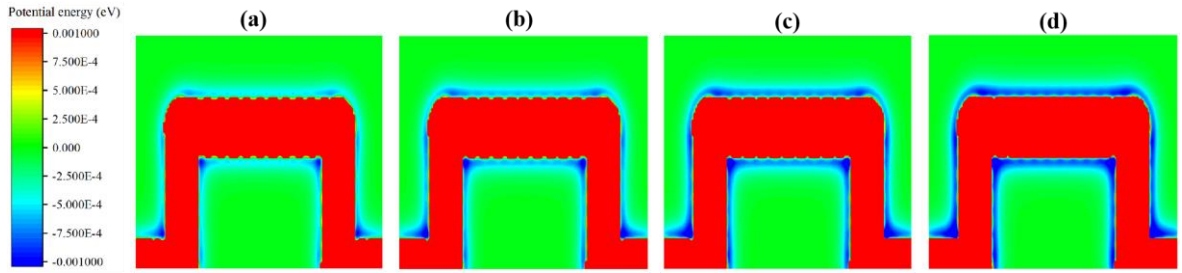

Fig. 8. The potential energy distribution along the nanopillar cross section under different fluid-solid interaction strengths. (a) *f* =1.0, (b) *f* =1.2, (c) *f* =1.4, (d) *f* =1.6.

4. Conclusions

In this paper, the condensation nucleation of water vapor on the copper surface with nanostructures was simulated by molecular dynamics. The effect of solid-liquid interaction strength on the nucleation characteristics at the early stage of frost formation was analyzed. The conclusions are summarized as follows:

As solid-liquid interaction strength increases, the condensate droplets evolve from Cassie to Wenzel state, which promotes the frosting process of the droplets. In particular, for *f*=1.4, the droplets form on the gap of nanopillars and undergo the transition from the Wenzel state to the Cassie state due to the combination of surface free energy and nanostructure. The effect of solid-liquid interaction strength on droplet wetting state was revealed from the perspective of potential energy distribution on the nanostructure surface. The area and value of the low potential energy region near the nanostructure surface increases with the solid-liquid interaction strength, which leading to the transition from Cassie state to Wenzel state.

Acknowledgements

This work is supported by the National Natural Science Foundation of China (52076036).

Nomenclature

Letters/Variables

q – charge

r – the distance between any two atoms

Greek symbols

σ – size parameter

ε – energy parameter

ε_0 – vacuum dielectric constant

References

[1] Wang, X., *et al.*, Stepwise optimization method of group control strategy applied to chiller room in cooling season, *Buildings*, *13* (2021), 2, pp. 487

[2] Wang, Z., *et al.*, Research on the characteristics of CO_2 heat pump integrated with thermal energy storage for space heating, *Journal of Mechanical Science and Technology*, *35* (2021), 5, pp. 2259-2270

[3] Hoque, M. J., *et al.*, Durability and degradation mechanisms of antifrosting surfaces, *ACS Applied Materials & Interfaces*, *15* (2023), 10, pp. 13711-13723

[4] Li, L., *et al.*, Investigation of defrosting water retention on the surface of evaporator impacting the performance of air source heat pump during periodic frosting – defrosting cycles, *Applied Energy*, *135* (2014), pp. 98-107

[5] Wang, F., *et al.*, Performance investigation of a novel frost-free air-source heat pump water heater combined with energy storage and dehumidification, *Applied Energy*, *135* (2015), pp. 212-219

[6] Hayashi, Y., *et al.*, Study of frost properties correlating with frost formation types, *Journal of Heat Transfer*, *99* (2022), 2, pp. 239-245

[7] Kondepudi, S., *et al.* Avoiding heat pump evaporator frosting through the use of desiccants, American Society of Mechanical Engineers, New York, NY (United States), 1995

[8] Kinsara, A. A., *et al.*, Proposed energy-efficient air-conditioning system using liquid desiccant, *Applied Thermal Engineering*, *16* (1996), 10, pp. 791-806

[9] Neinhuis, C., Barthlott, W., Characterization and distribution of water-repellent, self-cleaning plant surfaces, *Annals of Botany*, *79* (1997), 6, pp. 667-677

[10] Ma, J., *et al.*, Condensation induced delamination of nanoscale hydrophobic films, *Advanced Functional Materials*, *29*. (2019), 43, pp. 1905222

[11] Nouri, N., *et al.*, Effects of superhydrophobic, hydrophobic and hybrid surfaces in condensation heat transfer, *Journal of Applied Fluid Mechanics*, *14* (2021), 4, pp. 1077-1090

[12] Liu, T., *et al.*, Mechanism study of condensed drops jumping on superhydrophobic surfaces, *Colloids and Surfaces A: Physicochemical and Engineering Aspects*, *414* (2012), pp. 366-374

[13] Khatir, Z., *et al.*, Dropwise condensation heat transfer process optimisation on superhydrophobic surfaces using a multi-disciplinary approach, *Colloids and Surfaces A: Physicochemical and Engineering Aspects*, *106* (2012), 1, pp. 1377-1344

[14] Jin, X., *et al.*, Multifunctional engineering aluminum surfaces for self-propelled anti-condensation, *Advanced Engineering Materials*, *17* (2015), 7, pp. 961-968

[15] Hiratsuka, M., *et al.*, Molecular dynamics simulation of the influence of nanoscale structure on water wetting and condensation, *Micromachines*, *10* (2019), 9, pp. 587

[16] Liu, X., *et al.*, A study on the mechanism of water vapour condensation inhibition by nanostructures on the copper surface, *Journal of Materials Science*, *57* (2022), 44

[17] Fujii, A., *et al.*, Molecular dynamics simulation on effects of nanostructure on interfacial thermal resistance during condensation, *Journal of Thermal Science and Technology*, *15* (2020), 1, pp. JTST0010

[18] Wang, Z., *et al.*, Water vapour condensation on substrates with nanoscale hydrophilic spots: A molecular dynamics study, *International Journal of Heat and Mass Transfer*, *205* (2023), pp. 123929

[19] Paul, S., *et al.*, Role of wettability contrast on nanoscale condensation over hybrid wetting surface with gradient and patterned wetting configuration at various philic-phobic content, *Surfaces and Interfaces*, *36* (2023), pp. 102417

[20] Cui, C. B., Beom, H. G., Molecular dynamics simulations of edge cracks in copper and aluminum single crystals, *Materials Science and Engineering: A*, *609* (2014), pp. 102-109

[21] Abascal, J. L. F., Vega, C., A general purpose model for the condensed phases of water: TIP4P/2005, *The Journal of Chemical Physics*, *123* (2005), 23, pp. 234505
[22] Daw, M. S., Baskes, M. I., Embedded-atom method: Derivation and application to impurities, surfaces, and other defects in metals, *Physical Review B*, *29* (1984), 12, pp. 6443-6453
[23] Plimpton, S., Fast parallel algorithms for short-range molecular dynamics, *Journal of Computational Physics*, *117* (1995), 1, pp. 1-19
[24] Hiyama, M., *et al.*, Angular momentum form of verlet algorithm for rigid molecules, *Journal of the Physical Society of Japan*, *77* (2008), 6, pp. 064001
[25] Isele-Holder, R. E, *et al.*, Reconsidering dispersion potentials: Reduced cutoffs in mesh-based Ewald solvers can be faster than truncation, *Journal of Chemical Theory and Computation*, *9* (2013), 12, pp. 5412-5420
[26] Ruymgaart, A. P., Elber, R., Revisiting molecular dynamics on a CPU/GPU system: Water kernel and shake parallelization, *Journal of Chemical Theory and Computation*, *8* (2012), 11, pp. 4264-4236
[27] He, X., *et al.*, The Cassie-to-Wenzel wetting transition of water films on textured surfaces with different topologies, *Physics of Fluids*, *33* (2021), 11, pp. 1-8
[28] Gao, S., *et al.*, Tuning nanostructured surfaces with hybrid wettability areas to enhance condensation, *Nanoscale*, *11* (2019), 2, pp. 459-466

Paper submitted: 25 March 2025
Paper revised: 23 September 2025
Paper accepted: 24 September 2025